DOI: 10.13009/EUCASS2019-288

Numerical Analysis of Aerodynamic Instability for HAYABUSA Type Reentry Capsule

Toru TSURUMOTO, Yusuke TAKAHASHI, Hiroshi TERASHIMA and Nobuyuki OSHIMA
Hokkaido University, N13W8, Kita-ku, Sapporo, Hokkaido, Japan
tsuru-yeah@eis.hokudai.ac.jp
ytakahashi@eng.hokudai.ac.jp
htera@eng.hokudai.ac.jp
oshima@eng.hokudai.ac.jp

Abstract

Aerodynamic instability in the transonic flow regime is one of the critical problems, during atmospheric reentry phase using sample return capsule (SRC), which can cause self-excited oscillation by aerodynamic force. In this study, we numerically investigated flow fields around a Hayabusa-type SRC to clarify the mechanism of aero dynamic instability using a computational fluid dynamics (CFD) approach. Flow fields at subsonic and supersonic speeds in a transonic wind tunnel were reproduced here. The computed results indicated that an expansion region of the flow field is important to make the SRC stable.

1. Introduction

Several sample return missions, MMX, OKEANOS, and CAESAR, from the outer planets and their moons, have been proposed. Atmospheric re-entry is one of the inevitable phases in these missions. Development and design of sample return capsules (SRC) are strongly demanded.

During the atmospheric re-entry, aerodynamic instability for an attitude of SRC in flight is a critical problem. When the SRC has insufficient aerodynamic stability, the SRC can be oscillated and vertically rotated by the aerodynamic force. Then, the mission is suffered serious damage, e.g., landing at an unexpected place.

Hayabusa succeeded in sample return from the asteroid Itokawa in 2010. However, it was observed in wind tunnel experiments that the Hayabusa SRC has dynamic instability in the transonic regime, i.e., Mach number of 0.9 to 1.3. This means that the SRC's attitude is changed with its angular velocity in that experiment. Thus, the aerodynamic instability is strongly related to the SRC's motion. To prevent a decrease in aerodynamic performance, it is necessary to clarify the mechanisms of the attitude instability that is categorized as the static and dynamic instabilities [1]. The static stability is defined as that in which the force and moment act in the appropriate direction to return to the original balancing position when the vehicle's attitude changes. The static stability is only whether or not the restoring force or moment act to return to the original position. On the other hand, with respect to the dynamic stability, not only the restoring force and moment work, but also it is necessary to actually return to the original position. In other words, for the dynamic stability, the attitude motion should converge without divergence.

According to the previous study related to the Hayabusa-type SRC using the JAXA/ISAS transonic wind tunnel [2], it is indicated that inflow velocity is related to the SRC's motion. The study indicated that the SRC model freely rotated in an axis direction by the aerodynamic moment, and the angle-of-attack (AoA) was detected. Figure 1 shows the SRC model used in the previous study. In addition, Figs. 2 show time histories of AoA in the cases of Mach number of 1.1 and 0.7. It was indicated that the Hayabusa-type SRC becomes unstable in the transonic regime.

The other previous study using computational fluid dynamics (CFD) [3] concluded that the vortexes behind the SRC cause the phase delay of the base pressure against AoA and the phase delay makes the SRC unstable. However, it is possible that the turbulence model used in the study insufficiently reproduces various vortexes around the capsule. Hence, more detailed discussions about the effects of the vortexes will be required.

DOI: 10.13009/EUCASS2019-288

Mitigation of aerodynamic instability for the Hayabusa-type SRC is required yet in development and design for the new sample return missions. The present research objective is to investigate the mechanism of aerodynamic instability of the SRC. The CFD technique is used to obtain various data of the flow field, and the forced oscillation method is adapted to reproduce SRC motion. In addition, the large eddy simulation technique is used to resolve various vortexes around the SRC.

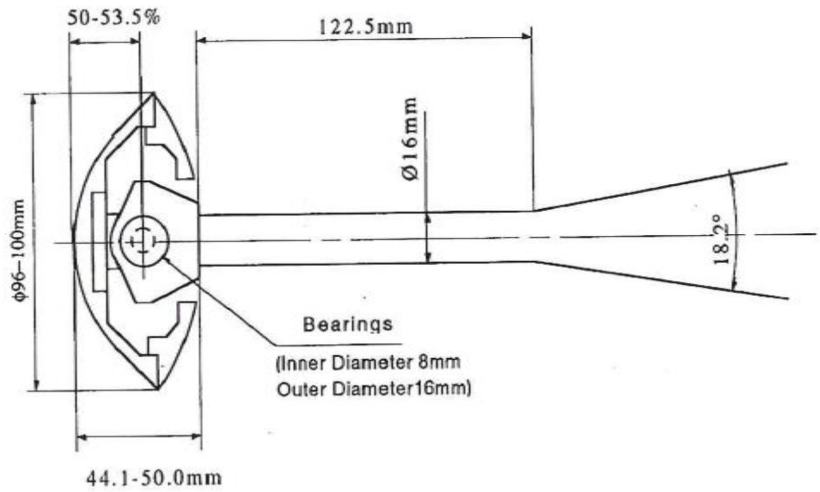

Fig. 1: Test apparatus [2]

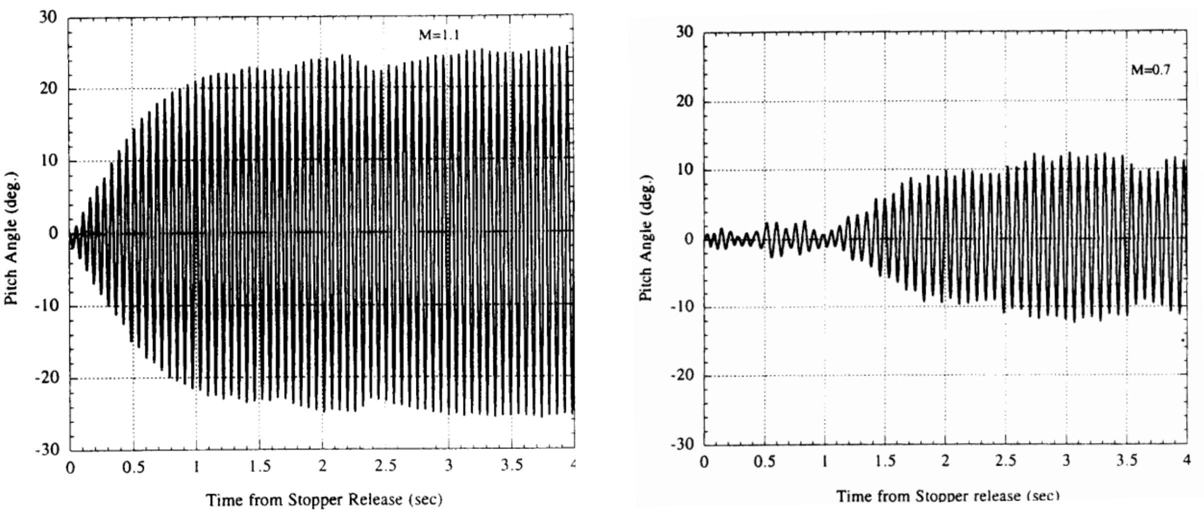

M1.1 M0.7

Figs. 2: Time histories of AoA of Hayabusa SRC in transonic wind tunnel [2]

2. Numerical analysis methods

Numerical simulations of Hayabusa-type SRC for cases of freestream Mach number of 1.1 and 0.7 are conducted to investigate dynamic instability. The compressive Navier-Stokes equations are adapted as the governing equation. RG-FaSTAR (version 2.1.6) [4] which is developed by JAXA and Hokkaido University is used as a flow field solver. Large-eddy simulation (LES) is adapted as a turbulence model. The Standard Smagorinsky model is adapted as the sub-grid scale model. The discretization method is the finite volume approach for an unstructured mesh. SLAU was used to evaluate the advection term, and higher-order accuracy for spatial direction was kept using the MUSCL method. The viscosity term is basically evaluated as the average between neighboring cells. The time integration method is LU-SGS. To reproduce the forced oscillation, angular velocity is given to the flux passing through the cell interface.

DOI: 10.13009/EUCASS2019-288

3. Analysis grid and analysis conditions

Figure 3 and 4 show the boundary conditions and computational grids used here, respectively. Uniform flow is given at the "Inflow" boundary. Zeroth-order extrapolation condition is imposed at the "Outlet" boundary. At the SRC surface, non-slip and isothermal wall are imposed. The surface temperature of SRC is fixed to 300 K. The number of cells is approximately 31 million. Table 1 shows the inflow flow conditions given at "Inflow". These conditions are the same condition as the previous study using the JAXA_ISAS transonic wind tunnel.

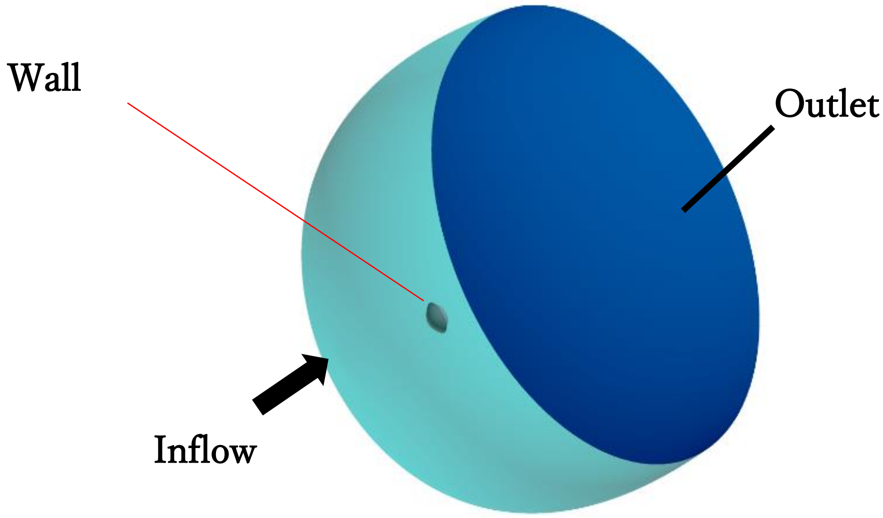

Fig. 3: Boundary conditions

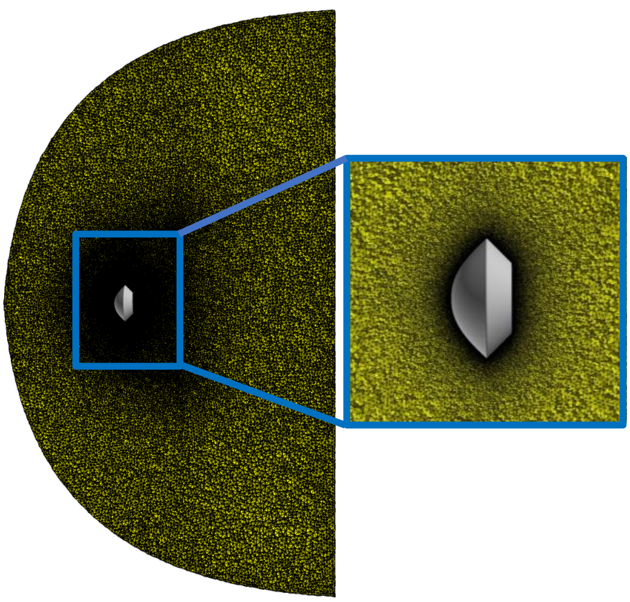

Fig. 4: Calculation grids

DOI: 10.13009/EUCASS2019-288

Tab. 1: Inflow conditions

Inflow Mach number	1.1	0.7
Inflow velocity [m/s]	342.8	232.1
Inflow temperature [K]	241.3	273.1
Inflow density [kg/m^3]	1.013	1.349
Inflow pressure [Pa]	7.02×10^4	1.08×10^5
Reynolds number	1.3×10^6	1.6×10^6

4. Result of static analysis

4.1 Validation in static analysis

Figure 5 shows a comparison of the pressure coefficient (Cp) distributions around the SRC surface between the numerical analysis and the experiment. Here, pressure coefficient, *Cp*, is given by the following equation:

$$Cp = \frac{p - p_\infty}{\frac{1}{2}\rho_\infty U_\infty} \quad (1)$$

where p is pressure and p_∞ is the inflow pressure. Though the front surface pressure reproduce the experiment results, rear surface pressure are underestimated. This is because of the sting behind the SRC in the experiment which is not reproduced on the present analysis. It was reported in Ref. [5] that the base pressure without sting is underestimated compared with the case with the sting. The present analysis result indicates the similar tendency with the previous result.

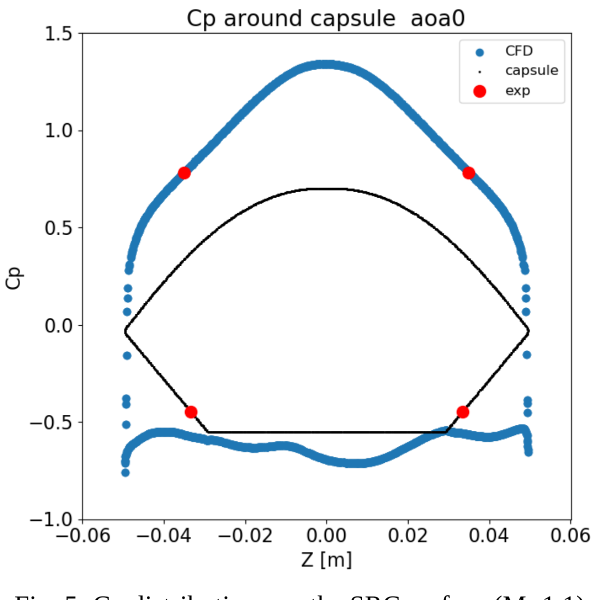

Fig. 5: Cp distributions on the SRC surface (M=1.1)

4.2 Static stability

Here, the static stability is referred to as an act of the restoring moment according to the displacement of the SRC attitude. The static stability is firstly evaluated to investigating aerodynamic stability.

In this study, the pitching moment coefficient (Cm) against AoA is used for evaluating the static stability, which is given by the following equation:

$$Cm = \frac{M}{\frac{1}{2}\rho_\infty U_\infty^2 Sl} \quad (2)$$

DOI: 10.13009/EUCASS2019-288

where M, ρ_∞, and U_∞ are the pitching moment, the inflow density, and the inflow velocity, respectively. And, S and l show the characteristic area and the characteristic length of the SRC, respectively. Figure 6 shows the definitions of positive/negative in Cm. The direction of the moment is defined as negative when the moment acts in the direction to restore the attitude with respect to the positive AoA. In other words, when the signs of the AoA and the pitching moment coefficient are different, the restoring moment acts on the capsule. Hence, Eq. (3) and (4) are given to keep the static stability as follows:

$$Cm < 0 \quad (when\ \alpha > 0) \tag{3}$$

$$\frac{\partial Cm}{\partial \alpha} < 0 \tag{4}$$

where, α means AoA.

Figure 7 shows the relation between Cm and AoA. This result satisfies Eq. (3) and (4). Thus, it is found that the SRC has static stability.

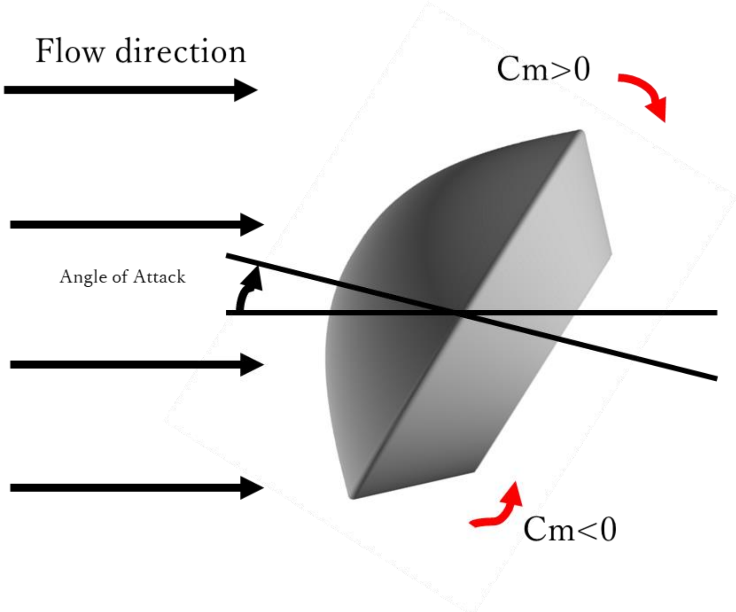

Fig. 6: Definition of positive/negative in Cm

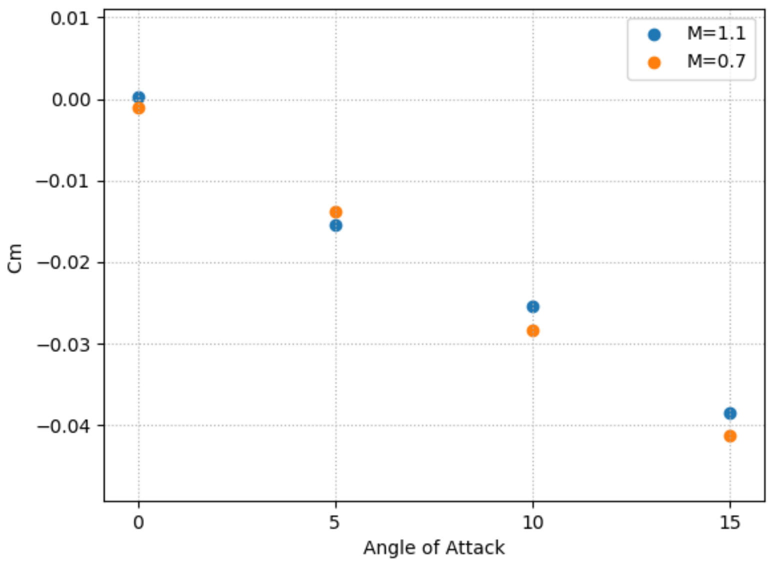

Fig. 7: Cm and AoA in the static analysis

DOI: 10.13009/EUCASS2019-288

5. Dynamic stability

As mentioned previously, it is indicated that the SRC has static stability in the transonic regime. Hence, the instability of the capsule attitude is possibly attributed to the effect of the capsule oscillation, i.e., dynamic stability. In this study, the oscillation of the SRC is numerically reproduced by the forced oscillation to investigate dynamic stability.

Table 2 shows the forced oscillation conditions used here. Reduced frequency is given by the following equation:

$$Reduced\ frequency = \frac{2\pi f D}{U_\infty} \tag{5}$$

where f is frequency and D is the diameter. The oscillation conditions are determined with reference to the previous wind tunnel tests [2].

Tab. 2: Forced oscillation conditions

Mach number	1.1	0.7
Frequency [Hz]	16	13
Amplitude [deg]	20	10
Reduced frequency [-]	0.030	0.035

Figures 8 show the Mach number distributions near the AoA of 0 deg obtained by the forced oscillation analysis. Figures 8-(a) and (c) are the case of Mach number of 1.1, and Figs. 8-(b) and (d) are the case of Mach number of 0.7. The SRC rotates in the clockwise direction in Figs. 8-(a) and (b), while rotates in the counterclockwise in Figs. 8-(c) and (d). Figures 9 show the relation of averaged Cm and AoA averaged over 15 cycles. The blue line means the rotation in the clockwise direction, and the red line means the counterclockwise.

Although there are differences in the flow field due to the difference in Mach number distributions obtained by the present computations, the difference between the clockwise and counterclockwise directions is not apparent at first glance from Figs.8. On the other hand, dynamic stability can be evaluated from Figs. 9. Figures 9 indicate that the SRC has dynamic instability when the Cm-AoA cycle is clockwise, while the SRC has dynamic stability when the Cm-AoA cycle is counterclockwise [6]. Consequently, the case of inflow Mach number of 1.1 is unstable. On the other hand, case of the inflow Mach number of 0.7 is stable. This corresponds to the results of the previous wind tunnel experiment [2]. The hysteresis shown in Figs. 9 means that there are dynamic effects acting the SRC, while the reason for the hysteresis is not obtained from Figs. 8 mentioned above.

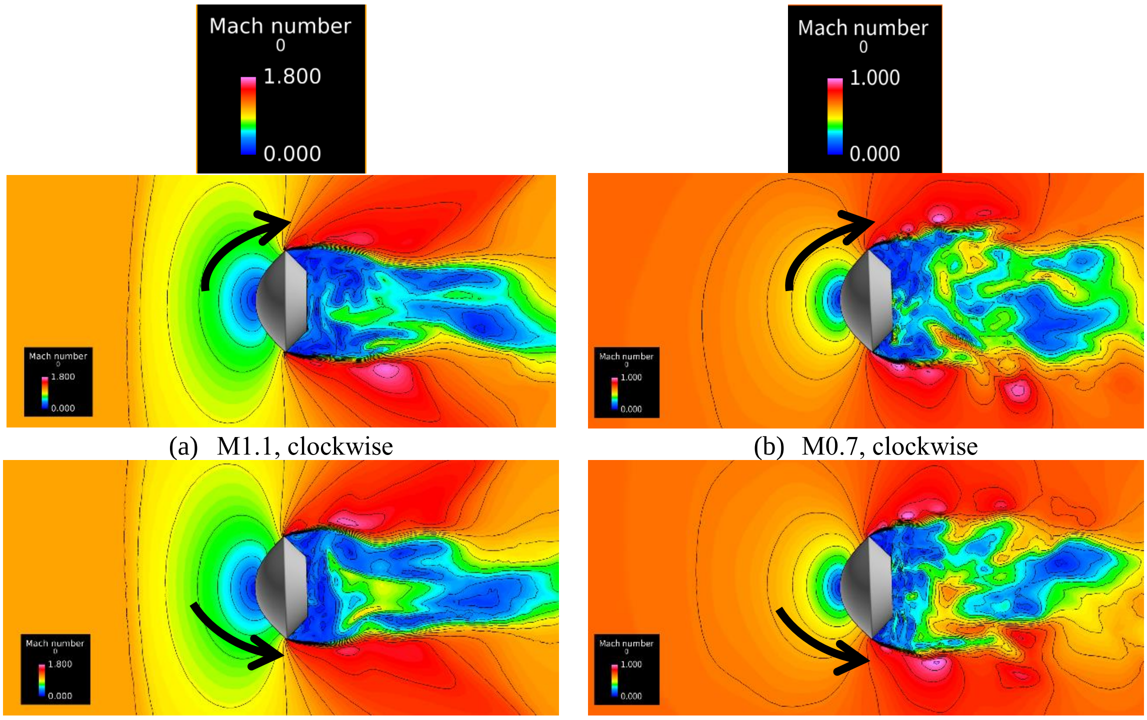

(a) M1.1, clockwise (b) M0.7, clockwise

(c) M1.1, counter clockwise (d) M0.7, counter clockwise

Figs. 8: Mach number distribution

DOI: 10.13009/EUCASS2019-288

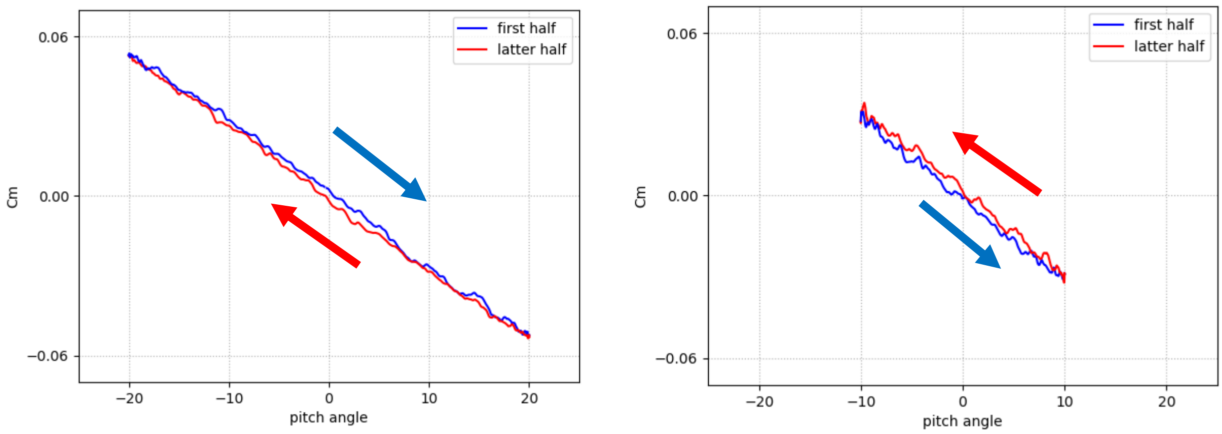

M1.1 M0.7

Figs. 9: Relation between Cm and AoA

Figures 10 show the relation between Cp and AoA at each point. The left side of Figs. 10 is the case of Mach number of 1.1, and the right side is the case of Mach number of 0.7.

As shown in Figs. 10-(a) and (c), it is possible that the dynamic instability for the case of Mach number of 1.1 is attributed to the hysteresis obtained at the front surface of the SRC. On the other hand, the effect of base pressure is low, and then, it is not the main reason although there appears slight hysteresis shown in Figs. 10-(e).

For the case of Mach number of 0.7, the base pressure has less dependence on AoA and no significant hysteresis is observed from Figs. 10-(e). Hence, the base effect is considered to be small. On the other hand, focusing on the front pressure, the hysteresis cannot be observed from Fig. 10-(b), while from Fig. 10-(d), the hysteresis can be observed around 0deg. The hysteresis that appeared in Figs. 10-(d) is consistent with the trend obtained in Fig. 9 and is considered to be the main factor that showed a stable trend at M0.7.

Then, comparing Fig. 10-(c) and Fig. 10-(d), even at the same point on the capsule surface, the hysteresis observed at a Mach number of 0.7 is reversed from that at a Mach number of 1.1, and it is considered to be reasons that changed the tendency of stability. For this reason, the difference in flow field around *point2* should be investigated.

Figures 11 show the time histories of the density gradient distribution at each Mach number. Focusing on *point2* shown in Figs. 10, for the case of a Mach number of 0.7, the fluctuation of the density gradient not seen at the time of a Mach number of 1.1 was observed. It seems that this fluctuation appears as the difference between Fig. 10-(c) and (d). Here, the area near point 2 is the expansion area of the SRC edge. When the shape of the SRC changes, the behavior of this part possibly also changes. In other words, it is thought that capsule design considering the dynamic stability should be performed by investigating the relation between the behavior of the expansion region of the capsule shoulder and the capsule shape at each Mach number.

DOI: 10.13009/EUCASS2019-288

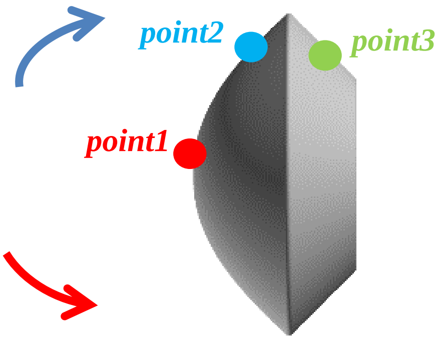

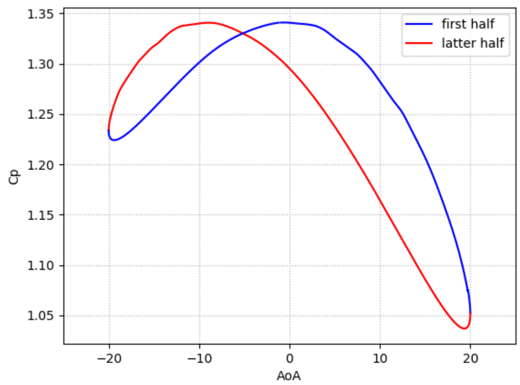

(a) M1.1, *point1*

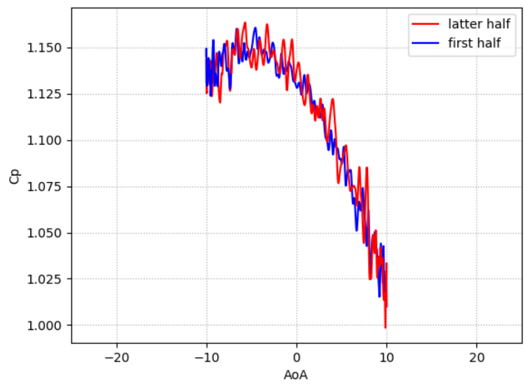

(b) M0.7, *point1*

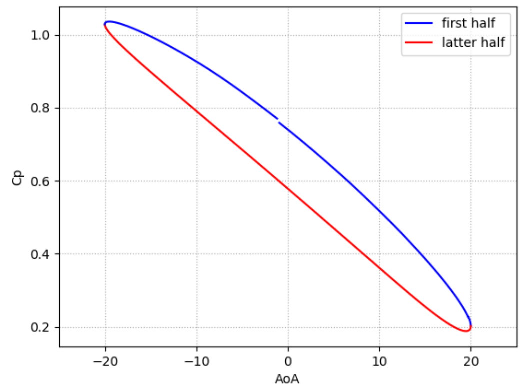

(c) M1.1, *point2*

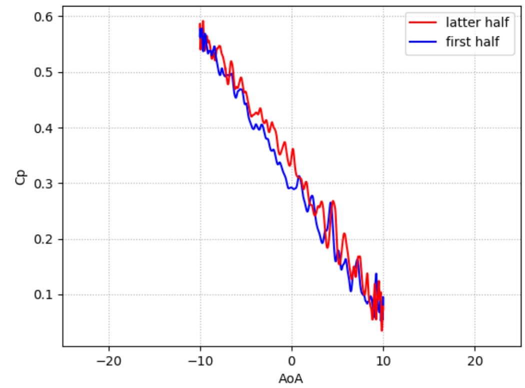

(d) M0.7, *point2*

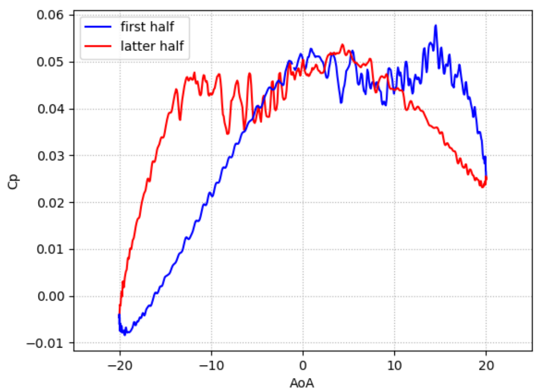

(e)M1.1, *point3*

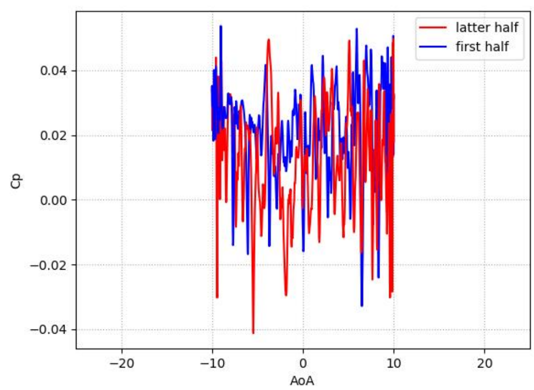

(f) M0.7, *point3*

Figs. 10: Relation between Cp and AoA at each point

DOI: 10.13009/EUCASS2019-288

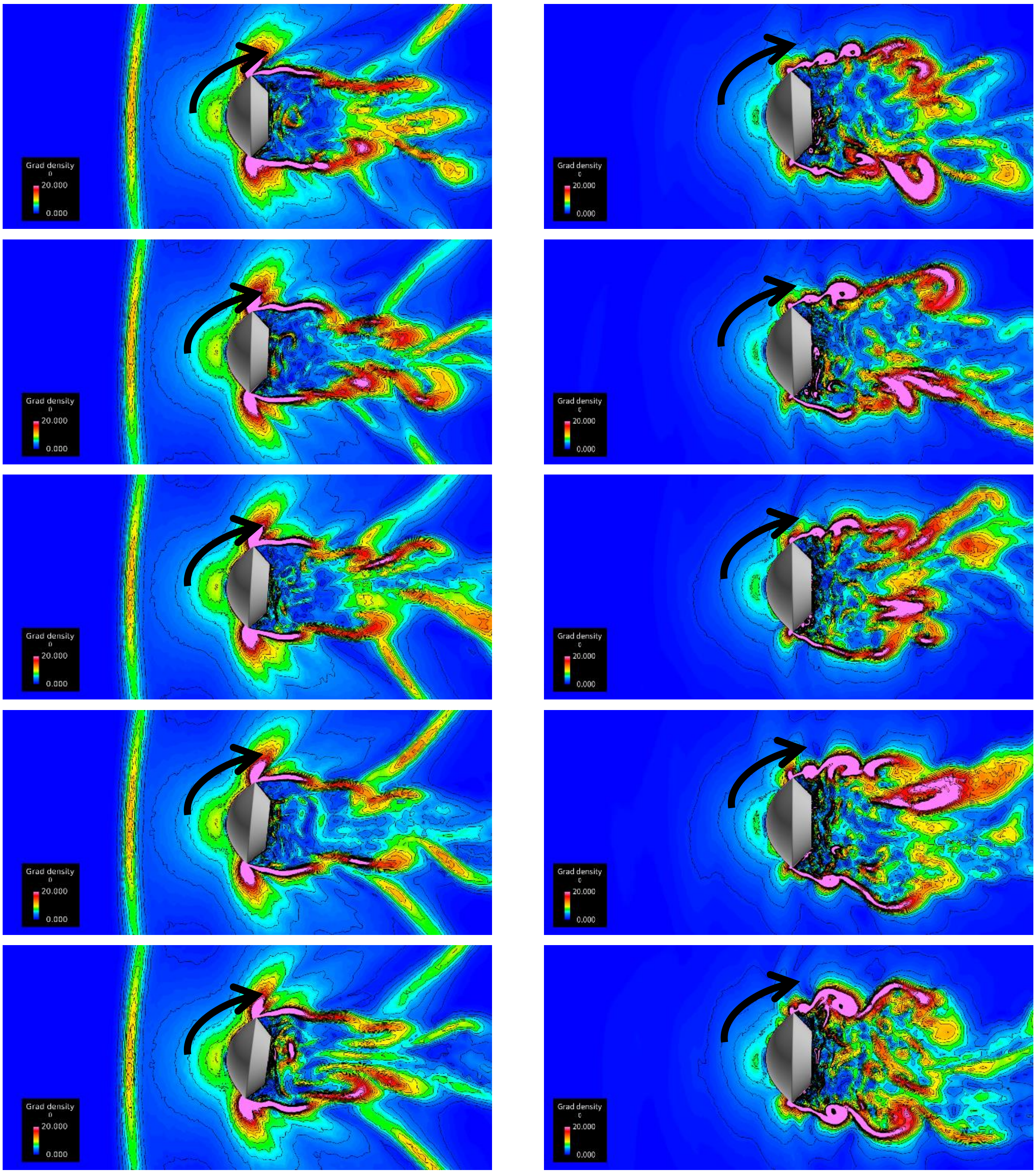

M1.1 M0.7

Figs. 11: Density gradient distribution

6. Conclusion

Numerical analyses using the forced oscillation method and the large eddy simulation technique were performed for two cases of inflow Mach number of 1.1 and 0.7 to investigate the mechanism of aerodynamic instability for the Hayabusa-type sample return capsule. As a result of the computations, it was found that the tendency of dynamic stability was reversed between the inflow conditions of the Mach number of 1.1 and 0.7. In addition, it was clarified that the cause is in the expansion area of the capsule shoulder. Hence, changing the shape of the capsule and comparing it with the behavior of the expansion area possibly lead to new insight into the design of the capsule for preventing the aerodynamic instability.

DOI: 10.13009/EUCASS2019-288

On the other hand, it is necessary to consider the relationship between the capsule shape and the behavior of the flow at the expansion area near the capsule shoulder in the future. Qualitative consideration was made from pressure history at a specific point in this study. However, in the future, it is required to quantitative evaluation considering the whole area of the SRC surface.

Acknowledgment

The present computational results were obtained using the fast unstructured CFD code "FaSTAR," which was developed by the Japan Aerospace Exploration Agency (JAXA). The computations were performed using the computational facilities at the Research Institute for Information Technology, Kyushu University.

References

[1] Tatsushi OHASHI, Yusuke TAKAHASHI, Hiroshi TERASHIMA and Nobuyuki OSHIMA, “Aerodynamic instability of flare-type membrane inflatable vehicle in suborbital reentry demonstration”, Journal of Fluid Science and Technology, Vol.13, No.3, 2018.

[2] Koju HIRAKI, Transonic Dynamic Instability of disk-shaped Capsule, The Institute of Space and Astronautical Science Report SP No.17(March 2003)

[3] Susumu Teramoto, Kozo Fujii. Mechanism of Dynamic Instability of a Reentry Capsule at Transonic Speeds. AIAA Journal, December 2002.

[4] Y. Takahashi, “Advanced validation of CFD-FDTD combined method using highly applicable solver for reentry blackout prediction”, Journal of Physics D: Applied Physics, Institute of Physics, Vol.49, No. 1, 2016, 015201 (15pp).

[5] Yusuke Takahashi, Manabu Matsunaga, Nobuyuki Oshima and Kazuhiko Yamada, “ Drag Behavior of Inflatable Reentry Vehicle in Transonic Regime”, Journal of Spacecraft and Rockets, Vol. 56, No. 2, March. 2019

[6] JoãoMonteiro, SébastienParis, LauraPeveroni, PatrickRambaud “ On the validation of experimental results for the dynamic stability of re-entry capsules” (2016).